Stress optical studies of drawn poly(ethylene methyl terephthalate)

M. A. O'Neill*, R. A. Duckett and I. M. Ward
Department of Physics, University of Leeds, Leeds LS2 9JT, UK
(Received 10 April 1987; revised 23 September 1987; accepted 28 September 1987)

Oriented tapes of poly(ethylene methyl terephthalate) (PEMT) and a 60/40 copolymer of PEMT and poly(ethylene terephthalate) (PET) have been prepared by drawing at different temperatures above and below the glass transition temperatures. It was established that in all cases the drawn samples showed no detectable crystallinity. The development of molecular orientation was characterized by birefringence and from the magnitude of the shrinkage force observed on heating above T_g. The results can be considered in terms of the deformation of a molecular network, without introducing complications due to crystallinity, and this was shown to provide a good first-order explanation for the data on drawing above T_g. Drawing below T_g, on the other hand, is better modelled by the pseudo-affine deformation scheme.

(Keywords: poly(ethylene methyl terephthalate); stress; optical measurements)

INTRODUCTION

Many studies have been made of the development of molecular orientation in poly(ethylene terephthalate) (PET) because of its technological importance in the oriented state. Structural techniques based on wide-angle X-ray scattering (WAXS)[1-3], optical birefringence[4-16], infra-red dichroism[16-22], polarized fluorescence[7-11,23], Raman spectroscopy[15,16,24,25] and nuclear magnetic resonance (n.m.r.) spectroscopy[26-28] have been used to measure the degree of molecular alignment in uniaxially oriented fibres and tapes and the degree of planar orientation of the phenyl groups in oriented film[1-3,28]. However, many of these studies have encountered problems because of uncertainties regarding the degree of crystallinity in the polymer and the way crystallinity changes with draw ratio. In this paper we describe studies of the development of molecular orientation in poly(ethylene methyl terephthalate) (PEMT), which previous work has indicated does not crystallize, either in the isotropic or in the drawn state[29]. PEMT is sufficiently similar to PET that many of the structural techniques previously used can be expected to be applicable, and the results may therefore be more readily interpretable without the problems associated with strain-induced crystallization. In order to bridge the gap between the two materials a non-crystallizing copolymer of PEMT and PET in the ratio 60:40 was also examined.

MATERIALS

Synthesis

PEMT was synthesized in our laboratories by the following route.

(*1*) *Oxidation of 1,2,4-trimethylbenzene.* Oxygen was passed through a solution of 1,2,4-trimethylbenzene in propionic acid in the presence of cobalt(II) bromide and manganese bromide tetrahydrate. The resulting solution was filtered hot to remove those acid products which are soluble in hot alcohol.

(*2*) *Esterification.* The two remaining acids (4-methylisophthalic acid and 2-methylterephthalic acid) were esterified using concentrated sulphuric acid in methanol to form dimethyl methyl terephthalate and dimethyl 4-methyl isophthalate. The former ester was then isolated by repeated recrystallization from methanol solution.

(*3*) *Ester interchange and polymerization.* An ester interchange was established between dimethyl methyl-terephthalate and ethylene glycol leading to a polycondensation polymerization in dimethyl phthalate at 282°C.

The absolute intrinsic viscosity of the resulting polymer was determined to be 0.67 by measuring the viscosity at three concentrations of the polymer in 2-chlorophenol. Two copolymers of PEMT/PET in the ratio 60:40 and 30:70 were made via a similar route, with intrinsic viscosities of approximately 0.58. Previous work by Edgar and Hill[28], who investigated the melting behaviour of several copolymers of PET, suggested that the crystallization window is at a minimum for the 60:40 ratio and so that copolymer was chosen for the following studies. This choice was confirmed by WAXS studies of isotropic and drawn fibres made from the two copolymers which revealed no trace of crystallinity. The glass transition temperatures were determined by d.s.c. at a scanning rate of 10 K min^{-1} and are shown in *Table 1*.

Production of oriented samples

Approximately 100 g was available of both PEMT homopolymer and the 60/40 PEMT/PET copolymer. With this in mind, and with the intention of producing samples suitable both for the stress-optical studies described here and for infra-red dichroism measurements

* Present address: ICI plc, Petrochemicals & Plastics Division, P.O. Box No. 90, Wilton, Middlesbrough, Cleveland TS6 8JE, UK

0032-3861/88/010054-07$03.00

Table 1

Polymer	T_g (°C)
PET	80
PEMT	61
30/70 PEMT/PET	72
60/40 PEMT/PET	68

PET, poly(ethylene terephthalate); PEMT, poly(ethylene methyl terephthalate); PEMT/PET, copolymer (with an appropriate molar composition as indicated)

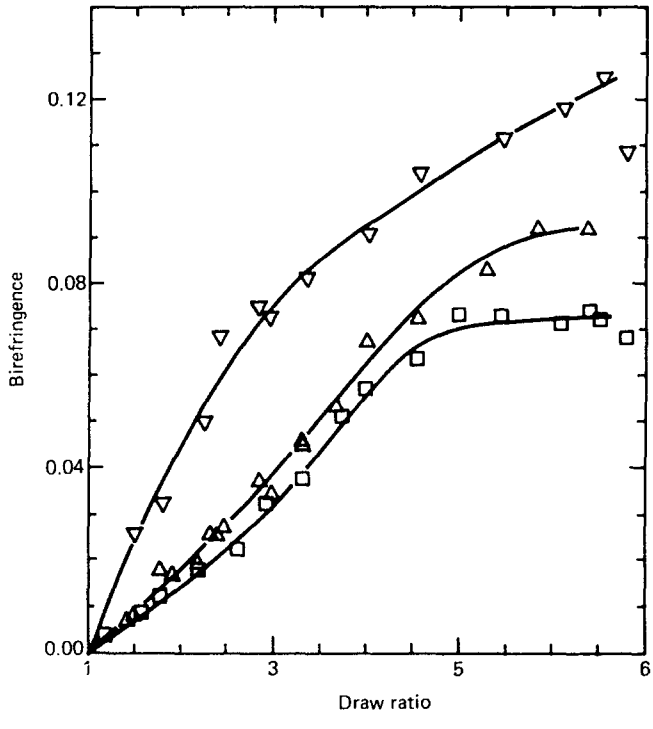

Figure 1 Birefringence *versus* draw ratio (λ) for homopolymer samples drawn at: ▽, 56; △, 65; □, 70°C

of molecular orientation and conformation to be described elsewhere, the following procedure was developed for producing oriented tapes.

To prevent degradation due to hydrolysis on heating, the polymer chips were dried under vacuum at 55°C for 24 h. They were then cooled under vacuum to room temperature and stored in a desiccator. Tapes of dimensions 25 μm × 1.0 mm wide were produced using a hydraulically operated rod-spinner operating at 200°C for PEMT and 180°C for the copolymer, in each case quenching the tape into a water bath 4 cm below the spinneret.

The isotropic tapes were then drawn using a conventional draw frame, the imposed draw-ratio being determined by the ratio of the surface speed of the draw-roll to that of the feed-roll. The drawing temperature was obtained by passing the polymer through a thermostatically controlled bath, which was about 15 cm long, positioned between the two rollers. The throughput of the tape resulted in a residence time of about 20 s in the heating medium (Dow-Corning silicone fluid, 200/1000 centistokes). This was a sufficiently long time to ensure that thermal equilibrium had been established. Draw temperatures of 56 and 70°C were used for the PEMT homopolymer, 63.5 and 75°C for the copolymer. Tests confirmed that the fluid chosen caused neither swelling nor plasticization of the polymer.

EXPERIMENTAL

Measurement of birefringence

The optical birefringence of each tape was measured with a Zeiss Interphako interference microscope using monochromatic light (wavelength 589 nm) to avoid problems due to dispersion. Samples cut with a wedge of 30° were immersed in a series of calibrated immersion liquids. The fringe shift was measured in each case between light passing through the sample and through an equal thickness of the known liquid. Graphs were constructed of the fringe shift against the corresponding refractive index of the liquid for the two orientations of the polarizer parallel and perpendicular to the draw direction.

The intercepts for zero fringe shift of the two parallel lines gave the two principal refractive indices from which the birefringence was deduced: the slope of the lines was used to calculate the specimen thickness. It was noted that Cargille liquids with refractive index above 1.628 caused the polymer to swell and so the range 1.63 to 1.72 was covered using aqueous solutions of mercuric potassium iodide, calibrated using an Abbe refractometer.

Measurement of shrinkage stress

The apparatus used was that described by Capaccio and Ward[29]. An oriented sample 8 cm in length was held at constant length and plunged into an oil bath at a temperature above the glass transition. Constraints on the sample length were not affected by thermal expansion of the apparatus. The force generated by the frustrated shrinkage of the sample was measured by a strain gauge dynamometer and the peak value recorded was used to calculate the shrinkage stress. Following previous work[30,12], a temperature of 8°C above T_g was chosen so that the peak value was attained in a few seconds.

RESULTS

The development of birefringence Δn with draw ratio for the PEMT homopolymer and the 60/40 PEMT/PET copolymer are shown in *Figures 1* and *2*. In some respects these results are similar to those obtained previously for PET[7-11,23]. For drawing at low temperatures (below T_g) the curves show a steep initial rise with a slope decreasing continuously with increasing draw ratio. The curves suggest a limiting value of birefringence for draw ratios greater than about five. For drawing at higher temperatures (above T_g) the birefringence/draw ratio curves are sigmoidal, again very similar to PET under similar conditions.

In another respect, however, the present results differ from those for PET. The value of maximum birefringence Δn_{max} appears to depend greatly on draw temperature and for both PEMT and the PEMT/PET copolymer it is lower than that for PET by a factor of about two.

The stress optical results are summarized in *Figures 3* and *4*. It can be seen that there is a linear relationship between the peak shrinkage stress and the birefringence which holds to the highest birefringences. This result is different from that obtained in PET, where the shrinkage

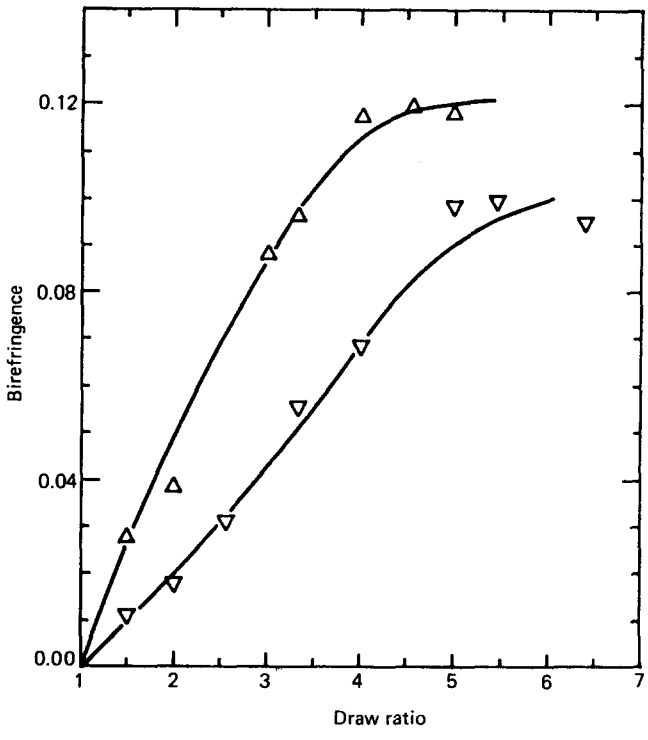

Figure 2 Birefringence *versus* draw ratio (λ) for PEMT/PET copolymer drawn at: ▽, 75; △, 63.5°C

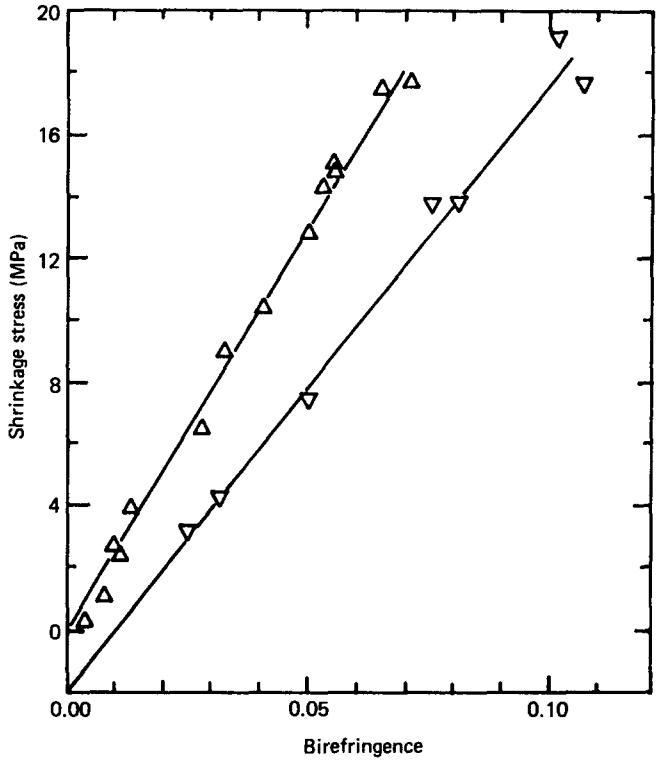

Figure 3 Shrinkage stress as a function of birefringence for PEMT samples drawn at 70 (△) and 56°C (▽) then subsequently shrunk at 70°C

stress rises linearly with birefringence only up to $\Delta n/\Delta n_{max} \leqslant 0.1$, subsequently reaches an intermediate plateau and then rises steeply again at very high birefringence[12].

DISCUSSION

Development of birefringence for drawing below T_g

At low temperatures the development of birefringence can be modelled by the pseudo-affine deformation scheme[31]. It is assumed that the optical anisotropy results from the orientation of anisotropic units, whose optical properties are identical to those of the fully oriented tape. The units are assumed to possess transverse isotropy and are characterized by α_3, the principal polarizability of the unit parallel to its symmetry axis, and α_1 the polarizability in the plane perpendicular to this axis. It is assumed that the symmetry axes of the units rotate as lines connecting pairs of points in a body undergoing uniaxial deformation at constant volume. The birefringence Δn is related to Δn_{max}, the maximum birefringence for a fully oriented sample by the relationship:

$$\frac{\Delta n}{\Delta n_{max}} = \frac{3\lambda^3}{2(\lambda^3-1)}\left[1 - \frac{1}{\sqrt{\lambda^3-1}}\sin^{-1}\frac{\lambda^3-1}{\sqrt{\lambda^3}}\right] - \frac{1}{2} \quad (1)$$

where λ is the draw ratio.

An initial calculation of Δn_{max} was made on the assumption that the structure of PEMT was similar to that of PET, the only difference being that one of the hydrogen atoms on the benzene ring is replaced by a methyl group. This was done using the bond polarizability data in *Table 2* (taken from refs 34–36) and

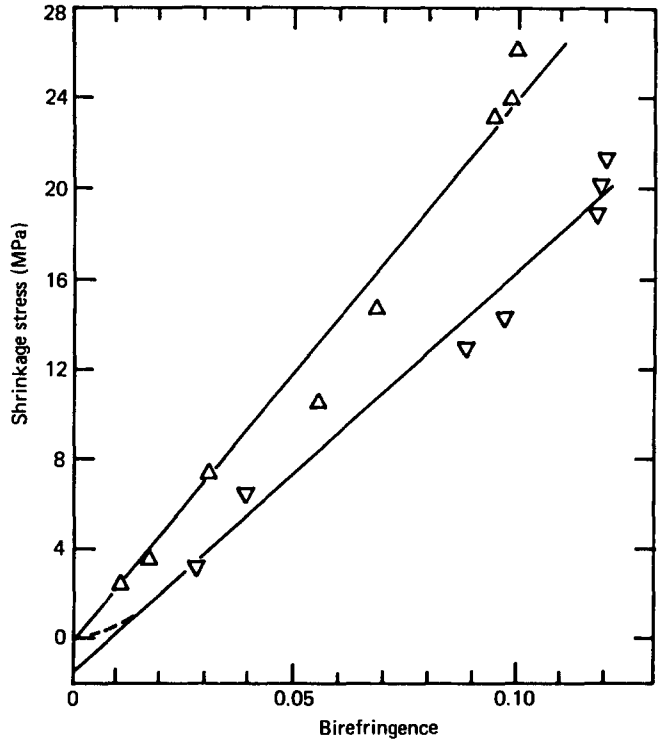

Figure 4 Shrinkage stress as a function of birefringence for PEMT/PET samples drawn at 75 (△) and 63.5°C (▽), then subsequently shrunk at 75°C

Table 2

Bond	Along bond (α_l)	Perpendicular to bond (α_t)
C–C	9.68	2.63
C–H	7.81	5.73
C–O	14.6	1.7
C=O	20.0	10.0
C(ar)–C	14.0	3.0
C(ar)–C(ar)	22.5	4.8

Bond polarizabilities $\times 10^{31}$ m^{-3}

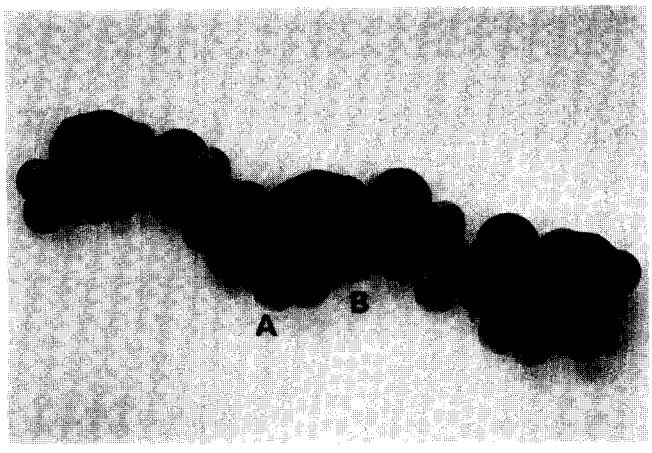

Figure 5 *Trans* configuration for PEMT showing the alternative positions A and B for the methyl group

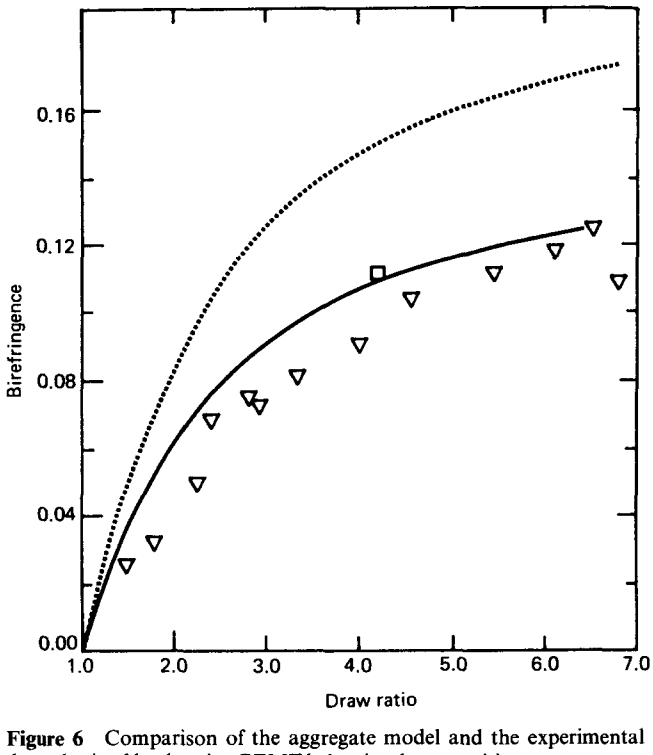

Figure 6 Comparison of the aggregate model and the experimental data obtained by drawing PEMT below its glass transition temperature: ▽, 56°C; □, 20°C. Δn_{max}: ----, 0.197; ——, 0.144

standard bond angles. As shown in *Figure 5*, there are two possible substitution positions, designated A and B. The average value for Δn_{max} for these two structures, with the additional assumption there is no steric hindrance to free rotation of the methyl group, was found to be 0.197. This value is clearly much greater than that indicated by the present data. By inspection of *Figure 6* a value of $\Delta n_{max} = 0.144$ can be seen to fit the birefringence data for this homopolymer. It is not possible at present to provide a theoretical understanding of this low value of birefringence but this is being attempted by computer modelling of possible molecular structures of PEMT.

The maximum birefringence for the PEMT/PET copolymer was calculated on the assumption that the contributions from PEMT and PET could be added on a simple proportionality basis 60:40 using the values 0.235 and 0.144 respectively. This gives a value of Δn_{max} of 0.169 for the copolymer, which can be seen from *Figure 7* to produce a good fit to the experimental results.

Development of birefringence for drawing above T_g

The drawing of PET above T_g has been modelled by the deformation of the rubber-like network. The initial part of the sigmoidal curve corresponds very well to the stretching of a rubber-like network, as can be seen from *Figures 8* and *9*, where the birefringence is plotted as a function of $-\lambda^2 - \lambda^{-1}$. Very good linear relationships were obtained for draw ratios less than about three, corresponding to the simple network model equation:

$$\frac{\Delta n}{\Delta n_{max}} = \frac{1}{5n}(\lambda^2 - \lambda^{-1}) \quad (2)$$

where n is the number of random links per chain.

This apparent simplicity does not, however, extend to the relationship between birefringence and draw ratio at high draw ratios. In this region a limiting birefringence is approached and it is of interest to examine these results in relation to the predictions of the modification of the rubber-network model proposed by Nobbs and Bower[10]. Their model contains the following assumptions.

(a) Any chain which becomes fully extended subsequently follows the pseudo-affine deformation scheme, rotating like a rigid rod.

(b) The end-to-end vectors of chains which were not fully extended continue to rotate and extend affinely.

No mechanism for how the transition from affine to pseudo-affine can occur was proposed. Nobbs and Bower showed that beyond the limiting draw ratio $\lambda > n^{1/2}$,

$$\frac{\Delta n}{\Delta n_{max}} = 1 - 128/(175x^{0.5}) \quad (3)$$

where $x = \lambda^2 n > 1$.

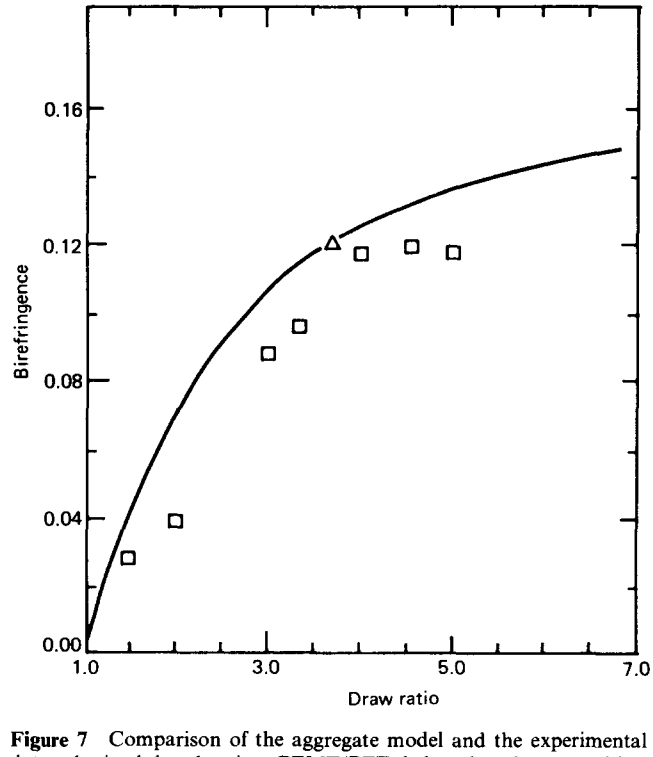

Figure 7 Comparison of the aggregate model and the experimental data obtained by drawing PEMT/PET below its glass transition temperature: △, 20°C; □, 63.5°C. ——, Aggregate model. $\Delta n_{max} = 0.169$

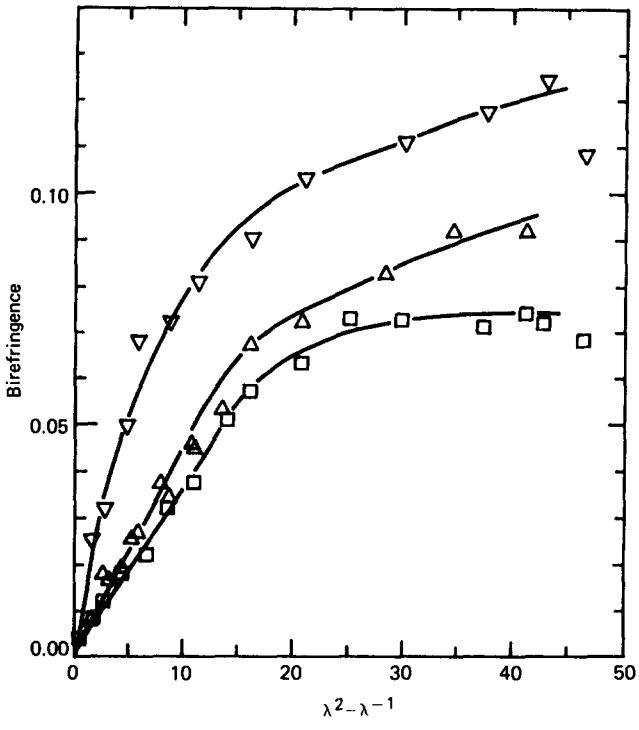

Figure 8 Birefringence *versus* $\lambda^2-\lambda^{-1}$ for PEMT samples drawn at: ▽, 56; △, 65; □, 70°C

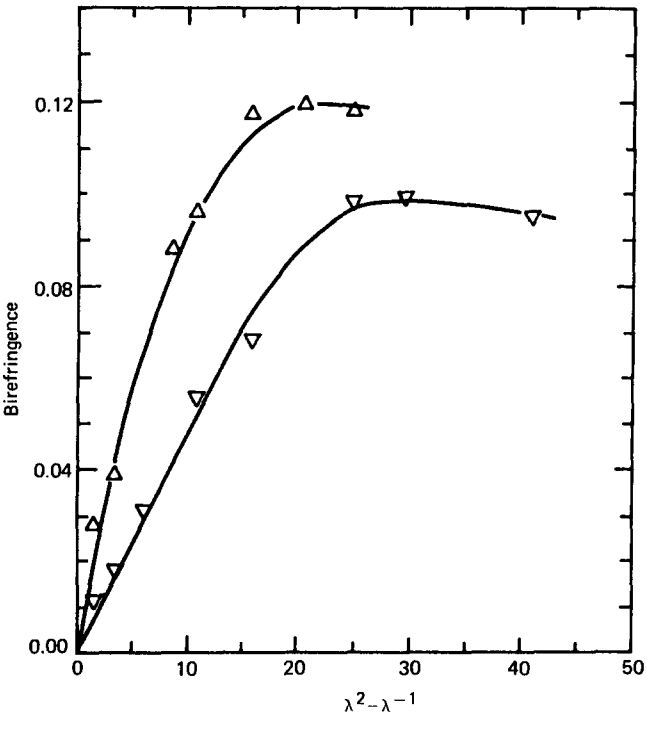

Figure 9 Birefringence *versus* $\lambda^2-\lambda^{-1}$ for PEMT/PET copolymer samples drawn at: ▽, 75; △, 63.5°C

It can be seen from *Figures 10*–12 that the predictions of the modified rubber network model are in qualitative agreement with the results for both PEMT and the PEMT/PET copolymer, the departure from conventional behaviour occurring at the value of $\lambda=n^{1/2}$ where n is determined by fitting the data for small λ only to equation (2).

Shrinkage stress

According to the Gaussian theory of rubber elasticity the stress supported by a network of N chains/unit volume at an absolute temperature T should vary with draw-ratio λ according to:

$$\sigma=NkT(\lambda^2-\lambda^{-1}) \quad (4)$$

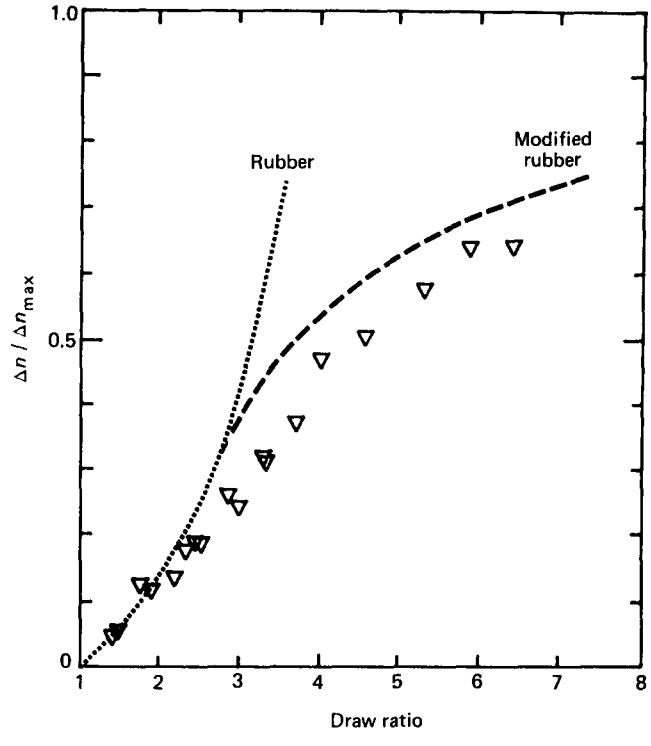

Figure 10 Comparison of the rubber model and the experimental data (▽) obtained by drawing PEMT at 65°C ($n=6.3$)

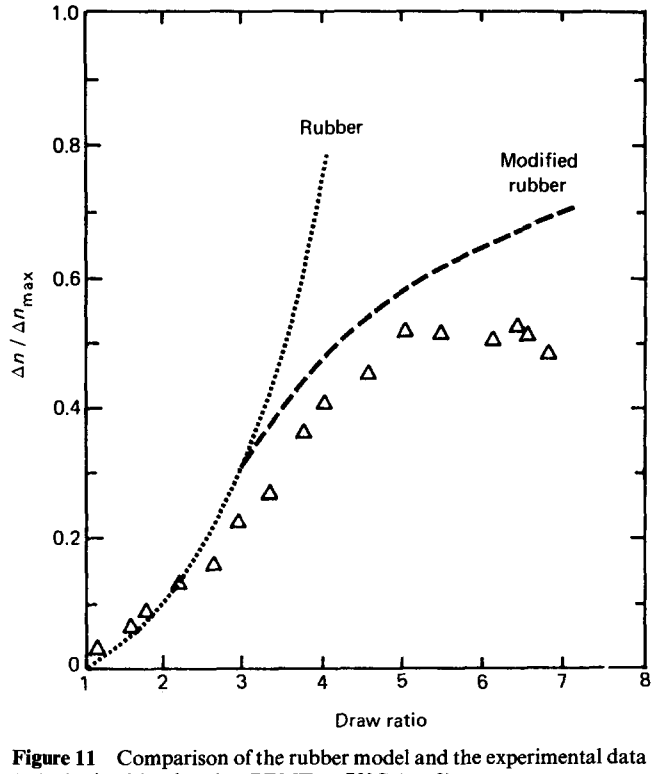

Figure 11 Comparison of the rubber model and the experimental data (△) obtained by drawing PEMT at 70°C ($n=8$)

Table 3

	PEMT		PEMT/PET	
Deformation temperature (°C)	56	70	63.5	75
Shrinkage temperature (°C)	70	70	75	75
Stress optical coefficient $(\Delta n/\sigma) \times 10^{-9} N^{-1} m^2$	5.19	3.56	5.57	4.10
Polarizability differences of the random link $(\alpha_1 - \alpha_2) \times 10^{29}$ m^{-3}	1.37	0.94	1.50	1.10
Number of monomers per link	3.37	2.31	3.30	2.43
Number of chains/unit volume ($\times 10^{-26}$ m^{-3})	3.35	2.15	3.05	2.49
Number of monomers/chain	11.5	18.0	13.0	16.0
Number of statistical links, n	3.4	8.0	3.9	6.6

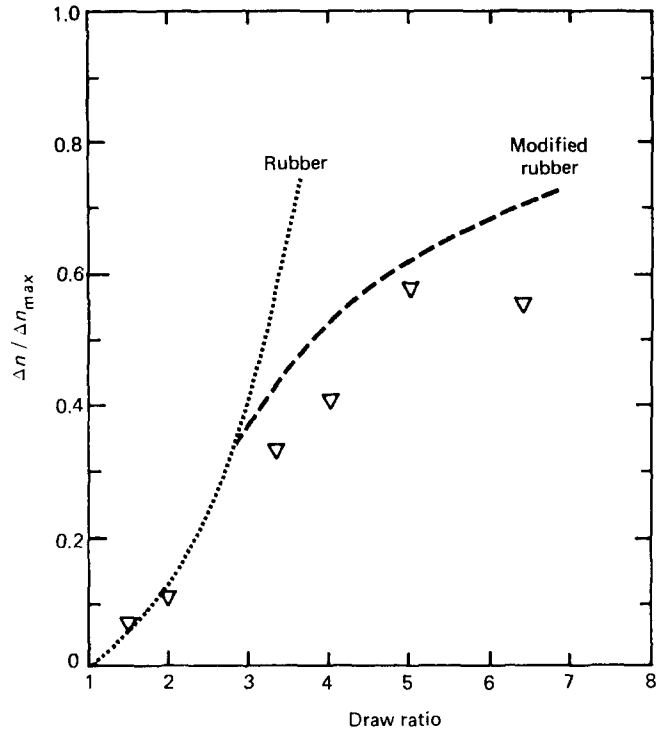

Figure 12 Comparison of the rubber model and the experimental data (▽) obtained by drawing PEMT/PET at 75°C ($n=6.6$)

At the same level of approximation the birefringence of the network is given by:

$$\Delta n = (2\pi/9\bar{n})(\bar{n}^2+2)^2 N(\alpha_1-\alpha_2)(\lambda^2-\lambda^{-1}) \qquad (5)$$

where $\bar{n}$ is the mean refractive index and $(\alpha_1-\alpha_2)$ is the difference in the principal polarizabilities of the equivalent random link. Equations (4) and (5) imply that a plot of Δn *versus* σ should be linear with a slope which is independent of N and λ, dependent only on the anisotropy of the random link. *Figures 3* and *4* are consistent with this representation over the whole range of λ. The simple behaviour observed in PEMT and the PEMT/PET copolymer compared with the more complex behaviour of PET[12] suggests that there is a constant stress-optical coefficient throughout, a result which may be due to the elimination of any crystallization.

Comparison of the data in *Figures 3* and *4* for samples drawn above and below T_g suggests, however, that the stress-optical coefficient, and therefore the equivalent random link, is a function of the drawing temperature. This result is in contrast with similar data recently obtained for PMMA where there does appear to be a unique stress-optical coefficient[35]. Similar data have not yet been obtained by homogeneously drawing PET below its T_g. The values of N, $(\alpha_1-\alpha_2)$ and n obtained from fitting the data from the homopolymer and the copolymer for λ in the range $1 \leqslant \lambda \leqslant 4$ are shown in *Table 3*.

In view of the uncertainty in the value of Δn_{max} for PEMT the values given in the table for the number of monomers per link and the number of statistical links n are subject to some uncertainty but it is unlikely that this is greater than about 10%. This does not substantially affect the comparisons which have been made.

Measurements of both shrinkage stress and birefringence from samples drawn to high λ reveal inadequacies in equations (4) and (5). It is interesting to note that these could formally be represented by allowing the parameter N to decrease significantly with increasing λ (at large λ), perhaps representing the slippage in the network required by a transition from affine to pseudo-affine deformation[10].

CONCLUSIONS

These studies have established that PEMT is a useful polymer for modelling the deformation of PET without the complications of crystallization. The birefringence and shrinkage stress data confirm that established theories of the deformation of a molecular network provide a first-order description to experimental observations for drawing above T_g. However, the behaviour at large λ is outside the scope of these simple theories and requires empirical modifications which are currently without justification from theory or direct observations at the molecular level. Drawing below T_g is better modelled by the pseudo-affine scheme with a limiting birefringence which indicates that the molecular configuration is dominated by the *cis*-conformation of the carbonyl groups.

REFERENCES

1 Dulmage, W. J. and Geddes, A. L. *J. Polym. Sci.* 1958, **31**, 499
2 Heffelfinger, C. J. and Burton, R. C. *J. Polym. Sci.* 1960, **47**, 289
3 Brown, N., Duckett, R. A. and Ward, I. M. *Philos. Mag.* 1968, **18**, 483
4 Allison, S. W. and Ward, I. M. *Br. J. Appl. Phys.* 1967, **18**, 1151
5 Purvis, J., Bower, D. I. and Ward, I. M. *Polymer* 1973, **14**, 398
6 Kashiwagi, M., Cunningham, A., Manual, A. J. and Ward, I. M. *Polymer* 1973, **14**, 11
7 Nobbs, J. N., Bower, D. I., Ward, I. M. and Patterson, D. *Polymer* 1974, **15**, 287
8 Bhatt, G. M. and Bell, J. P. *J. Polym. Sci., Polym. Phys. Edn* 1976, **14**, 575
9 Nobbs, J. N., Bower, D. I. and Ward, I. M. *Polymer* 1976, **17**, 25
10 Nobbs, J. N. and Bower, D. I. *Polymer* 1978, **19**, 1100

11 Nobbs, J. N., Bower, D. I. and Ward, I. M. *J. Polym. Sci., Polym. Phys. Edn* 1979, **17**, 259
12 Rietsch, F., Duckett, R. A. and Ward, I. M. *Polymer* 1979, **20**, 1133
13 Perena, J. M., Duckett, R. A. and Ward, I. M. *J. Appl. Polym. Sci* 1980, **25**, 1381
14 Bower, D. I. and Ward, I. M. *Polymer* 1982, **23**, 645
15 Bower, D. I., Jarvis, D. A. and Ward, I. M. *J. Polym. Sci., Polym. Phys. Edn*, in press
16 Jarvis, D. A., Hutchinson, I. J., Bower, D. I. and Ward, I. M. *Polymer* 1980, **21**, 41
17 Farrow, G., McIntosh, J. and Ward, I. M. *Makromol. Chem.* 1960, **36**, 147
18 Schmidt, P. G. *J. Polym. Sci. (A)* 1963, **1**, 1271
19 Koenig, J. L. and Cornell, S. W. *J. Macromol. Sci. (B)* 1967, **1**(2), 279
20 Cunningham, A., Ward, I. M., Willis, H. A. and Zichy, V. *Polymer* 1974, **15**, 749
21 Padibjo, S. R. and Ward, I. M. *Polymer* 1983, **24**, 1103
22 Nobbs, J. N., Bower, D. I., Ward, I. M. and Patterson, D. *Polymer* 1974, **15**, 287
23 Purvis, J., Bower, D. I. and Ward, I. M. *Polymer* 1973, **14**, 398
24 Purvis, J. and Bower, D. I. *J. Polym. Sci., Polym. Phys. Edn* 1976, **14**, 1461
25 Boyce, C. A. and Goodlet, V. W. *J. Appl. Phys.* 1963, **34**, 59
26 Slonim, I. Ya and Urman, Y. G. *Zh. Struht. Khin* 1963, **34**, 216
27 Farrow, G. and Ward, I. M. *Polymer* 1960, **1**, 330
28 Edgar, O. B. and Hill, R. *J. Polym. Sci.* 1951, **8**, 1
29 Capaccio, G. and Ward, I. M. *Colloid Polym. Sci.* 1982, **260**, 46
30 Pinnock, P. R. and Ward, I. M. *Trans. Faraday Soc.*, 1966, **62**, 1308
31 Ward, I. M. *Proc. Phys. Soc.* 1962, **80**, 1176
32 Denbigh, K. G. *Trans. Faraday Soc.* 1940, **36**, 936
33 Bunn, C. W. 'Chemical Crystallography', Oxford University Press, London, 1961, p. 312
34 Bunn, C. W. and Daubeny, R. de P. *Trans. Faraday Soc.* 1954, **50**, 1173
35 Botto, P. A., Duckett, R. A. and Ward, I. M. *Polymer* 1987, **28**, 257